JEM

Coordinated oncogenic transformation and inhibition of host immune responses by the PAX3-FKHR fusion oncoprotein

Stephen Nabarro,[1] Nourredine Himoudi,[1] Antigoni Papanastasiou,[1] Kimberly Gilmour,[2] Sian Gibson,[3] Neil Sebire,[3] Adrian Thrasher,[2] Michael P. Blundell,[2] Mike Hubank,[1] Glenda Canderan,[1] and John Anderson[1]

[1]Unit of Molecular Haematology and Cancer Biology and [2]Unit of Molecular Immunology, Institute of Child Health, London WC1N 1EH, England, UK
[3]Department of Histopathology, Great Ormond Street Hospital for Children, London WC1N 3JH, England, UK

Tumors have evolved elaborate mechanisms for evading immune detection, such as production of immunoinhibitory cytokines and down-regulation of major histocompatibility complex (MHC) expression. We have studied PAX3–FKHR as an example of an oncogenic fusion protein associated with an aggressive metastatic cancer. We show that PAX3–FKHR alters expression of genes that are normally regulated by Janus kinase/signal transducer and activator of transcription (STAT) signaling pathways. This occurs as a result of a specific interaction between PAX3–FKHR and the STAT3 transcription factor, which results in a dramatic reduction in tumor MHC expression, and an alteration in local cytokine concentrations to inhibit surrounding inflammatory cells and immune detection. Collectively, these data show that an oncogenic transcription factor can promote tumor growth and tissue invasion while inhibiting local inflammatory and immune responses. This is the first time that an immunomodulatory role has been described for an oncogenic fusion protein.

CORRESPONDENCE
John Anderson:
j.anderson@ich.ucl.ac.uk

Abbreviations used:
CM, conditioned medium;
4HT, 4-hydroxy-tamoxifen;
RMS, rhabdomyosarcoma;
siRNA, small interfering RNA;
TAP, transporter associated with antigen processing.

Rhabdomyosarcoma (RMS) is an aggressive tumor resembling developing skeletal muscle that predominantly affects children (1). PAX3-FKHR is an oncogenic fusion protein and is specifically associated with the alveolar subtype of RMS (ARMS), which is a more aggressive tumor than the embryonal form (ERMS) that lacks PAX3-FKHR and is less likely to be metastatic or locally invasive (2–5). PAX3-FKHR can transform NIH3T3 cells and chicken embryo fibroblasts (6, 7), whereas experimentally induced expression of PAX3-FKHR in ERMS cells has been shown to result in more rapid tumor growth and local tissue invasion (8). PAX3-FKHR has recently been shown, when expressed in mouse Myf6 expressing developing myoblasts, to promote formation of tumors that histologically and immunohistochemically resemble human ARMS (9). PAX3-FKHR contains the NH_2-terminal DNA binding domain of PAX3 fused in frame with the COOH-terminal transactivation do-

main of FKHR. PAX3-FKHR confers strong transcriptional activation of known PAX3 target genes mediated by the FKHR transcriptional activation domain (10–12).

A component of cancer progression is the failure of the host immune response to recognize tumor cells. STATs are a family of transcription factors that are activated by tyrosine phosphorylation in response to a variety of growth factors and cytokines. Specifically for IFN-γ, signaling occurs through IFN-γ receptor subunits 1 and 2 (IFN-γR1 and -2), which interact with JAK1 and JAK2 and predominantly activate STAT1. For IL-6, the IL-6 receptor interacts predominantly with JAK1 and predominantly activates STAT3 (13). The STATs undergo homo- and heterodimerization, bind DNA, and induce expression of target genes. Moreover, there is cross talk between IL-6 and IFN-γ signaling; e.g., IL-6 will trigger an IFN-γ response predominantly via STAT1 in the absence of STAT3 (14, 15). Recently, aberrant activation of STAT3 has been recognized in a variety of human cancers to cause a negative regulation of inflammatory responses and an inhibition of cross talk between innate and adaptive immu-

S. Nabarro, N. Himoudi, and A. Papanastasiou contributed equally to this work.

The online version of this article contains supplemental material.

JEM

nity, thereby allowing unrestrained tumor growth (16–18). STAT3 activation as a primary oncogenic event has not, however, been described and has been assumed to result from deregulation of upstream kinases and growth factors.

We provide evidence that a primary transforming oncogenic event (generation of PAX3-FKHR fusion protein) also contributes to tumor immune escape through a novel interaction with STAT3. The presence of the PAX3-FKHR–STAT3 complex alters transcription of known STAT target genes, causing an immunoinhibitory tumor environment.

RESULTS
PAX3–FKHR induces transcriptional activation and repression in RMS cells

To investigate how PAX3-FKHR fusion alters gene expression, we transfected two different ERMS cell lines (RD and 76-9) with PAX3-FKHR and generated stable clones. 76-9 are murine RMS cells (19) that form tumor xenografts that resemble the embryonal histological type and express the myogenic marker MyoD1 (unpublished data). RD is a human ERMS cell line. PAX3-FKHR protein activity in 76-9 and RD stable clones was quantified in transient transfection assays. Six clones (76–9–P3F-C23, 76–9–P3F-C24, and RD-P3F clones 2, 5, 6 and 18) were chosen and showed levels of PAX3-FKHR protein activity of ∼30% of the level of SCMC-RM2 and RH30, cell lines that both endogenously express PAX3-FKHR (Fig. 1 A).

We have previously shown that transfecting RD cells with *PAX3-FKHR* results in enhancement of locally invasive tumor growth in vivo (8). In matrigel invasion assays, 76–9–P3F-C23 and 76–9–P3F-C24 cells were significantly more invasive than control vector transfected 76-9 (P < 0.005; Fig. 1 B). Therefore, ectopic PAX3-FKHR expression causes a phenotypic change in ERMS cells consistent with the more aggressive phenotype of ARMS. PAX3-FKHR transcriptional targets in 76-9 cells were determined by oligonucleotide microarray gene expression analysis. 31 genes were significantly up-regulated and 69 genes were down-regulated by PAX3-FKHR (P < 0.05 by *t* test; see Table I for a summary; for a complete gene list, see Tables S1 and S2, available at http://www.jem.org/cgi/content/full/jem.20050730/DC1). For three genes tested (*pai*, *xmr*, and *crabp1*), the expression changes in Northern blot analysis were equivalent to those seen in microarrays (Fig. 1 C). We were further convinced of the validity of the gene list because of the up-regulation of *IGF2*, a known PAX3-FKHR target gene that is frequently overexpressed in RMS (20–22) and was induced five- to sixfold by PAX3-FKHR in 76-9 cells (Table I).

PAX3-FKHR down-regulation of target genes in human and murine cells

To determine if the transcriptional targets for PAX3-FKHR that we had detected in 76-9 cells were similarly regulated in a different cellular environment, we investigated expression
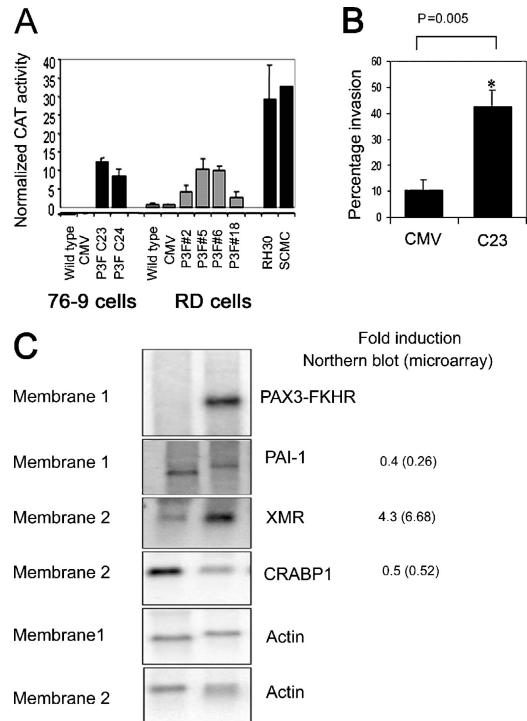

Figure 1. PAX3–FKHR causes both up- and down-regulation of target genes. (A) PAX3-FKHR protein function in 76-9 and RD cells stably transfected with pBK-CMV-P3F as determined by transient transfection assays using the specific PAX3 reporter plasmid PRS-9 linked to CAT. This contains six direct repeats of the *PAX3* paired domain and homeodomain consensus sequences upstream of a *CAT* reporter. CAT activity is plotted in arbitrary units ± SEM of triplicate samples. This assay is representative of four separate experiments. (B) Matrigel invasion assay to show that PAX3-FKHR increases the invasive ability of 76-9 cells. Percent invasion was calculated as: (number of invasive cells / total number of cells) × 100. Mean values ± SEM of quadruplicate samples are plotted. PAX3-FKHR–expressing 76–9–P3F-C24 cells (and 76–9–P3F-C23 cells; not depicted) were significantly more invasive than 76–9–CMV cells. *, P < 0.005 by *t* test. Data are representative of three separate experiments. (C) Northern blot analysis of vector (CMV) and PAX3-FKHR–transfected (C23) 76-9 cells. (right) Fold changes in mRNA expression in C23 relative to CMV are shown for the Northern blots (and the microarrays). (left) Two replica blots were probed. Band intensities were normalized relative to actin.

patterns of two down-regulated genes (*PAI-1* and *MHC class 1*) in human ERMS (RD) cells stably transfected with *PAX3-FKHR*. Although PAX3-FKHR causes only a modest reduction in *MHC class1* mRNA, the presence of the fusion completely abrogated its surface expression in RD as well as in 76-9 cells (Fig. 2 A), possibly because of the concurrent inhibition of transporter associated with antigen processing (TAP) transcription (Table I). PAI-1 inhibits tissue invasion by inhibiting urokinase plasminogen activator, which is involved in RMS cell migration (23), and we have previously shown that RD cells transfected with *PAX3-FKHR* have enhanced tissue invasion (8). In agreement with data generated in the murine cells, RD cells (wild type or

Table I. Genes significantly up- and down-regulated more than twofold by PAX3-FKHR in 76-9 cells

Gene	GenBank accession number	Affymetrix identity code	Description	CMV fold change	C23 fold change	C24 fold change	p-value
IGF2	X71922	98623_g_at	Insulin-like growth factor 2	1	5.02	6.03	<0.001
PLA2	AA408341	94665_at	Phospholipase A2 group 5	1	3.74	4.44	<0.001
PLA2	U66873	101328_at	Phospholipase A2 group 5	1	3.70	3.05	0.002
TGOLN2	D50032	93882_f_at	Trans-Golgi network protein 2	1	2.33	2.22	<0.001
XMR	X72697	102818_at	Xlr-related, meiosis regulated gene	1	6.88	7.19	<0.001
CSTF2T	AI854864	104126_at	Cleavage stimulation factor, 3′ pre-RNA subunit	1	2.06	2.36	0.002
TRAM1	AA763937	160936_at	Translocating chain-associating membrane protein 1	1	2.65	2.89	<0.001
AKR1C13	AB027125	95015_at	Aldo-keto reductase family 1, member C13	1	2.13	3.08	<0.001
COL3A1	X52046	98331_at	Collagen α I, type 3 subunit	1	3.31	4.06	<0.001
IFN-regulated genes							
G1P2	X56602	98822_at	IFN-α–inducible protein	1	0.25	0.20	<0.001
IFI204	M31419	98465_f_at	IFN-activated gene 204	1	0.15	0.11	<0.001
ISGF3G	U51992	103634_at	IFN-stimulated gene factor 3 γ	1	0.23	0.17	<0.001
H2-K	V00746	93120_f_at	MHC class I, histocompatibility 2, K region	1	0.49	0.49	0.002
H2-D1	X52490	101886_f_at	Histocompatibility 2, D region locus 1 and β(2) microglobulin	1	0.59	0.5	0.003
TAP1	U60020	103035_at	Transporter associated with antigen processing 1	1	0.42	0.46	0.003
CXCL10	M33266	93858_at	Chemokine (C-X-C motif) ligand 10 (IFN-inducible protein 10)	1	0.36	0.25	0.001
STAT1	U06924	101465_at	Signal transducer and activator of transcription 1	1	0.31	0.41	0.004
CCL5	AF065947	98406_at	Chemokine ligand 5 (regulated on activation, normal T cell expressed and secreted)	1	0.41	0.26	0.002
Additional genes							
CRABP1	X15789	98108_at	Cellular retinoic acid binding protein 1		0.52	0.41	0.002
PAI1	M33960	94147_at	Plasminogen activator inhibitor 1	1	0.26	0.34	0.001

Data are presented as expression level relative to the parental cell line (CMV). The expression level of each target gene is set as 1 in the CMV cells. The values for each cell line are the means of three probe arrays. The GenBank/EMBL/DDBJ accession numbers from which the oligonucleotide sequences were drawn are shown. p-values were determined by t test.

vector transfected) expressed high levels of PAI-1 protein, but the presence of PAX3-FKHR caused a dramatic reduction, and cell lines endogenously expressing PAX3-FKHR had low PAI-1 protein (Fig. 2 B).

Interestingly, a large proportion (29 out of 69) of the genes repressed by PAX3-FKHR in the microarray screen were known target genes of STAT1 and/or STAT3 that were regulatable by IFN-γ and/or IL-6 via JAK/STAT signaling cascades. (Table I and Tables S1 and S2) (24). We postulated that PAX3-FKHR might function in part by inhibition of transcription downstream from IL-6 and/or IFN-γ receptors. We began by confirming that MHC class I and PAI-1 were IFN-γ targets in RD cells (Fig. 2, C and D). In RD cells transfected with PAX3-FKHR, addition of IFN-γ did induce MHC expression, but the maximal expression

was significantly less than was seen in vector-transfected cells (Kolmogorov-Smirnov test between RD-P3F#6 + IFN-γ and RD-CMV + IFN-γ, P < 0.001; Fig. 2 C). More strikingly, there was no substantial increase in PAI-1 after addition of IFN-γ in the presence of PAX3-FKHR (Fig. 2 D). The effect of PAX3-FKHR on PAI-1 protein in RD cells was mirrored in changes at the RNA level, where the presence of PAX3-FKHR completely abrogated IFN-γ response (Fig. 2 E). Of note, the IFN-γ targets down–regulated by PAX3-FKHR in Table I have known roles of inhibition of tumor growth through generation of inflammatory responses (e.g. CXCL10, CCL5, MHC, and TAP). We reasoned that if interference with transcription downstream from IFN-γ/ IL-6 signaling was a function of PAX3-FKHR, then genes that are normally inhibited by IFN-γ should be up-regulated
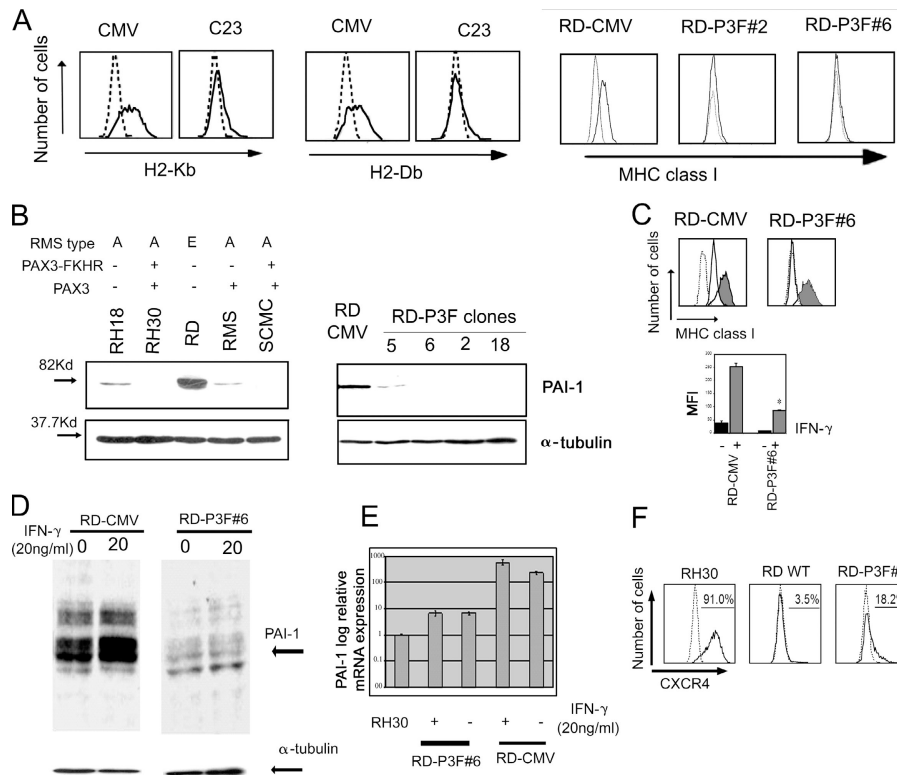
JEM

Figure 2. PAX3–FKHR substantially down–regulates PAI–1 and MHC class I protein expression in mouse and human RMS cells. (A) FACS analysis of MHC class I surface expression. The dotted line represents the secondary antibody alone, and the continuous line represents staining with anti–MHC class I. The staining is representative of four separate experiments. (B) Western blot analysis examining PAI-1 protein expression in RD-CMV and RD-P3F clones and in several human RMS cell lines. In a longer exposure, very faint bands can be detected in the lanes corresponding to the RD-P3F clones 6, 2, and 18. The RMS type and the expression of endogenous *PAX3* and *PAX3-FKHR* RNA (determined by Northern blot; not depicted) for each cell line is indicated. A, ARMS; E, ERMS. (C) FACS analysis of MHC class I surface expression on cells cultured in the presence of 20 ng/ml IFN-γ for 48 h. The dotted line represents the secondary anti-body alone, the continuous line represents MHC class I expression in the absence of IFN-γ, and the shaded histogram represents MHC class I in the presence of 20 ng/ml IFN-γ. FACS staining is representative of three separate experiments. Mean fluorescence intensities from the FACS plots are also indicated. Error bars = SEM. (D) Western blot of PAI-1 expression after treatment with 20 ng/ml IFN-γ for 48 h is representative of two independent experiments. PAI-1 was detected at a molecular mass of ~47 kD, and α-tubulin expression was used as a loading control. (E) PAI-1 expression determined by quantitative RT-PCR. Expression is normalized to GAPDH and expressed relative to RH30 expression. Error bars = SEM of triplicate estimations. (F) FACS histograms of CXCR4 surface expression. The dotted line represents isotype control antibody, and the continuous line represents anti-CXCR4 antibody.

by PAX3-FKHR and contribute to tumor progression. This was found to be true for the chemokine receptor CXCR4 (Fig. 2 F), confirming the previously recognized role for this protein in promoting ARMS metastasis downstream from PAX3-FKHR (25).

PAX3-FKHR interacts physically with STAT3 to modify STAT3 transcription

We hypothesized that PAX3-FKHR might interact with STAT3 because (a) STAT3 plays a critical role in immune evasion in tumor cells (17); (b) it down-regulates the proinflammatory cytokines CCL5 (regulated on activation, normal T cell expressed and secreted) and IP10 that we show to be down-regulated by PAX3-FKHR (17); and (c) FKHR itself has recently been shown to interact with STAT3 and to be a transcriptional coactivator for it (26). Moreover, be-

cause most ARMS tumors express a fusion gene with PAX3 or PAX7 fused in frame with a FOXO1 family member (27), we reasoned that FKHR is likely to contribute to the function of PAX3-FKHR over and above its contribution of a strong transcriptional activation domain.

We initially investigated a putative interaction with STATs by using a 4-hydroxy-tamoxifen (4HT)–inducible estrogen receptor–tagged PAX3-FKHR construct stably transfected in RD cells (Fig. 3 A). After addition of 4HT, the estrogen receptor antibody coimmunoprecipitated STAT3 and PAX3-FKHR in RD cells expressing PAX3-FKHR–ER (Fig. 3 B) but did not precipitate STAT3 in the absence of 4HT or in RD cells transfected with an empty vector (not depicted). Interestingly, in the absence of 4HT, the anti-STAT3 antibody repeatedly failed to immunoprecipitate STAT3 in PAX3-FKHR–ER–transfected RD cells (Fig. 3

B), even though STAT3 could readily be precipitated from vector-transfected RD cells (not depicted). This suggested that cytoplasmic PAX3-FKHR–ER might sequester STAT3 in the cytoplasm in an inaccessible form. To determine the region of PAX3-FKHR that interacts with STAT3, we generated myc epitope–tagged full-length PAX3-FKHR and truncated PAX3 lacking all of the FKHR components of the fusion. These myc-tagged fusions were transiently transfected into 293T cells, and high-level expression was obtained (Fig. 3 C, left). After transfection with full-length PAX3-FKHR, both myc and STAT3 antibodies were reproducibly able to immunoprecipitate STAT3, but this coimmunoprecipitation could not be performed in untransfected 293T cells or in 293T cells transfected with truncated PAX3 (Fig. 3 C). The

interaction was specific for STAT3 because STATs 2, 4, and 6 failed to coprecipitate with PAX3-FKHR (Fig. 3, right). However in both RD and 293T cells transfected with PAX3-FKHR, precipitation of PAX3-FKHR weakly coprecipitated STAT5, suggesting a weak interaction between these proteins (Fig. 3, B and C). To confirm that this interaction also occurs in ARMS cell endogenously expressing PAX3-FKHR, we were able reproducibly to coimmunoprecipitate PAX3-FKHR and STAT3 in RH30 cells that endogenously express PAX3-FKHR (Fig. 3 D). The intensity of the STAT3 band immunoprecipitated by the PAX3 antibody in Fig. 3 D appears weaker than that precipitated by the myc epitope antibody in Fig. 3 C because the PAX3 antibody is very inefficient at immunoprecipitation.
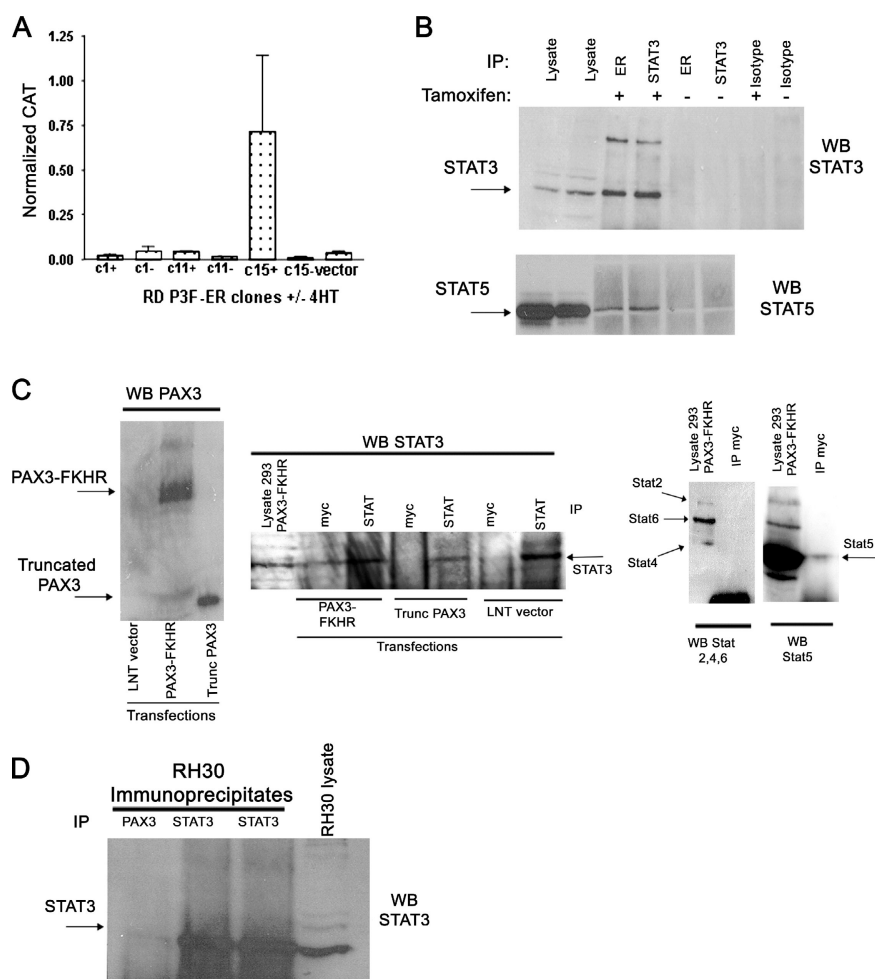

Figure 3. PAX3–FKHR interacts with STAT3. (A) Transient transfection assay using PRS9-CAT reporter showing specific inducible activity of PAX3-FKHR in clone 15 on addition of 4HT. Error bars = SEM of triplicate transfections. (B) Coimmunoprecipitation of STAT3 with estrogen receptor–tagged PAX3-FKHR is seen only in presence of 4HT. The IP is representative of three separate experiments. The high molecular mass band of ∼200 kD shown here was not seen in all replicate experiments. (bottom) Replica blot probed with STAT5. (C) Immunoprecipitations from 293T cells transfected with PAX3-FKHR, truncated PAX3-FKHR lacking FKHR regions, or empty vector. (left) Lysates are detected with an anti-PAX3 antibody. Immunoprecipitates are detected with an anti-STAT3 antibody. The IP data are representative of three separate experiments. (right) Replica blots from the same transfections probed with antibodies against STATs 2 (113 kD), 4 (81 kD), 5 (95 kD), and 6 (100 kD). No staining with STATs 2, 4, or 6 was observed when the membrane was subject to longer exposures. (D) Coimmunoprecipitation experiment to show that an anti–NH$_2$ terminus PAX3 antibody and anti-STAT3 antibody are both able to precipitate STAT3 from RH30 cells. The blot is representative of two independent experiments.

JEM

The presence of PAX3–FKHR causes the STAT3–dependent generation of immunoinhibitory secreted factors

We hypothesized that the range of altered transcription induced by PAX3-FKHR that we had identified might make the tumor environment more immunoinhibitory. We used DC activation/maturation as a marker of the tumor cytokine environment. For these experiments, we collected conditioned medium (CM) from PAX3-FKHR–expressing and –non-expressing cell lines grown in the presence or absence of a specific phosphopeptide inhibitor of activated STAT3 (28). Human DCs were generated from monocytes in the presence of CM, and activation was determined by flow cytometry after staining with HLA-DR and CD86. CM from RD cells stably transfected with estrogen-tagged PAX3-FKHR (RD-P3FER clone 15) inhibited DC activation only after addition of 4HT. This inhibition was STAT3 dependent because the
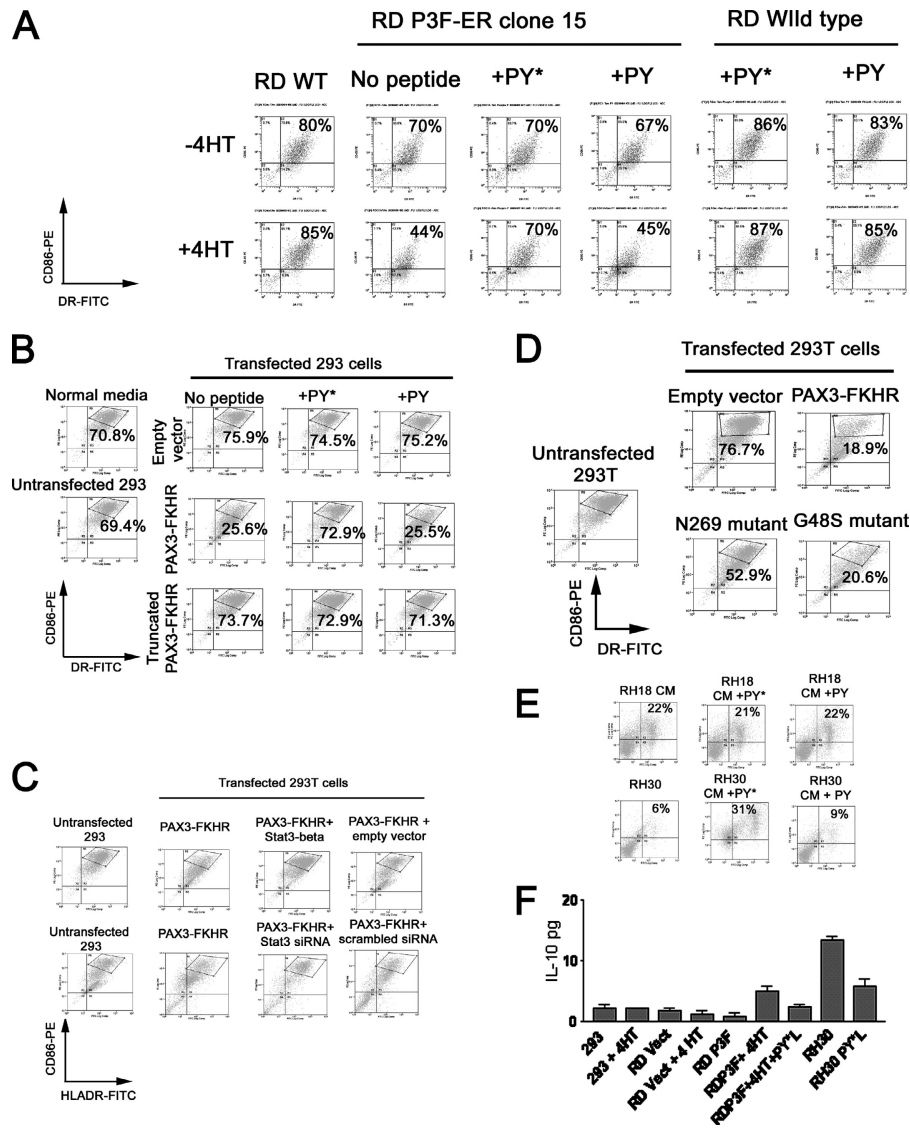

Figure 4. **The presence of PAX3–FKHR causes the STAT3–dependent generation of immunoinhibitory secreted factors.** (A–E) Flow cytometric analysis of HLA-DR and CD86 expression on viable CD11c^{+}-gated DCs generated in CM from various cell lines (RD Vect$^{+/-}$ 4HT and RD P3F-ER$^{+/-}$ 4HT; 293T transfected with combinations of empty vector, truncated PAX3, PAX3-FKHR, PAX3-FKHR mutants, dominant negative STAT3, or siRNA against STAT3; and RH18 or RH30) 24 h after KLH activation. As indicated, conditioned media were obtained after growth of cell lines in the presence of a specific STAT3 inhibitory phosphopeptide (PY*) or control nonphosphorylated peptide (PY). G48S, paired domain mutant PAX3-FKHR; N269, homeodomain mutant of PAX3-FKHR; STAT3-β, dominant-negative form of STAT3. Data are the representative result of between two and three independent experiments. Conditioned media were collected from confluent cell lines 48 h after passaging. All FACS plots have logarithmic scales. Percentages refer to the percentage of CD11c-positive cells in the top right quadrant or indicated gates. (F) Stat-3 expression in tumor cells increases IL-10 cytokine production. Detection of human IL-10 secretion in tumor cells expressing inducible P3F-ER. Results are presented as the SEM of triplicate samples and are representative of two independent experiments.

effect was completely lost in the presence of the phosphopeptide inhibitor but not an unphosphorylated control peptide (Fig. 4 A). Moreover, the inhibition was specific for PAX3-FKHR because CM from vector transfected RD cells was unaffected by 4HT and anti-STAT3 phosphopeptide in terms of the ability to inhibit DC activation (Fig. 4 A). To assess whether this PAX3-FKHR effect could be reproducibly demonstrated in a different cell environment, we analyzed CM from 293T cells transiently transfected with full-length or truncated PAX3-FKHR (see Fig. 3 C for levels of expression of transfected proteins). Expression of full-length but not truncated PAX3-FKHR almost completely inhibited DC activation, and this inhibition was STAT3 dependent because it was completely reversed by the specific phosphopeptide in-

hibitor but not by control peptide (Fig. 4 B). We next confirmed that the inhibitory effects of the phosphopeptide inhibitor could be repeated using other methods of specific STAT3 down-regulation. Both cotransfection with small interfering RNA (siRNA) targeting STAT3 and STAT3-β (a dominant-negative form of STAT3) (17, 29) specifically and completely prevented PAX3-FKHR–mediated inhibition of DC maturation (Fig. 4 C). We hypothesized that if PAX3-FKHR were interacting with STAT3 through the FKHR component of the fusion, then its effect on DC maturation might be independent of transcription of PAX3 target genes. To test this, we transfected 293T cells with mutant forms of PAX3-FKHR containing point mutations in the paired domain (G48S) and homeodomain (N269) (6, 30). The paired
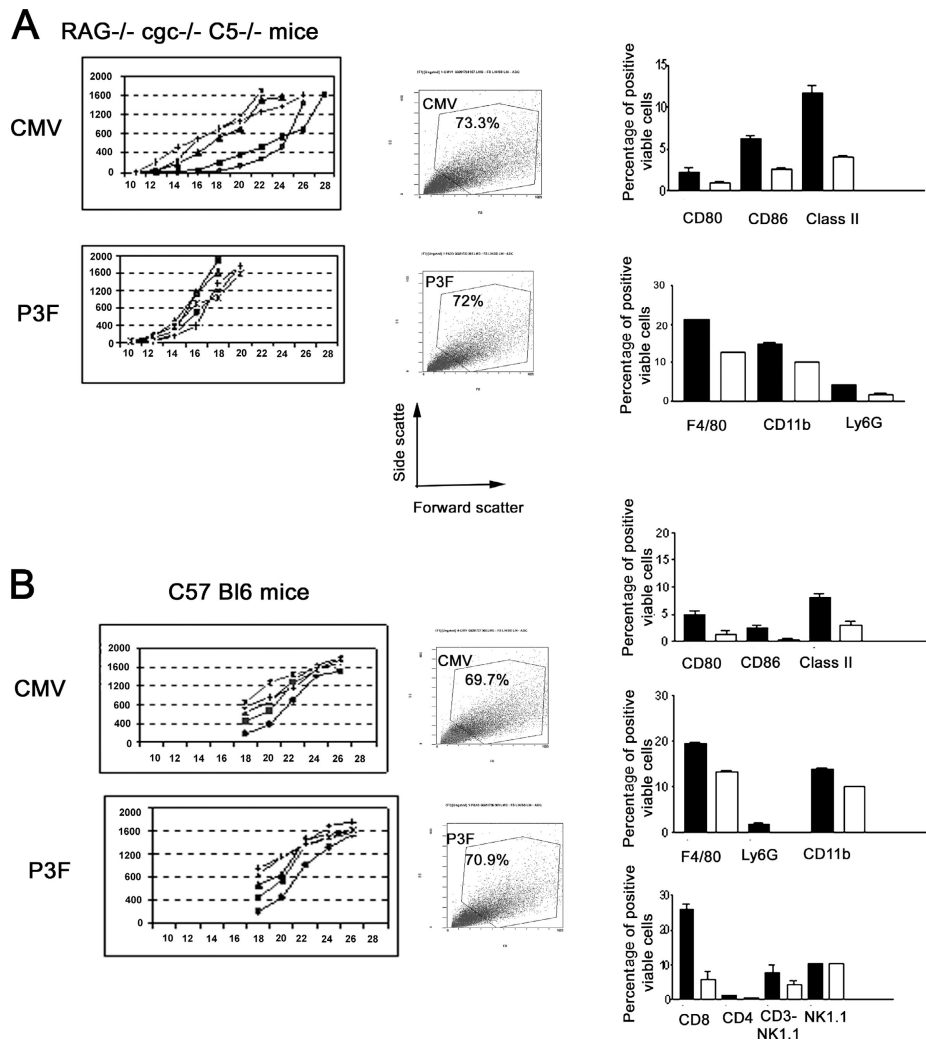

Figure 5. PAX3–FKHR suppresses local inflammatory and immuno-logical responses and causes more rapid in vivo growth rate in immunodeficient mice. Tumor growth rates and tumor infiltrating cells of PAX3-FKHR expressing (C23) or control (CMV) cells grown in immuno-deficient (A) or syngeneic C57BL/6 (B) mice. Each line represents the tumor growth curve of an individual animal. Tumor-infiltrating cells were deter-mined by FACS analysis. Histograms indicate the percentage of total cells that were gated as viable cells for the analysis of tumor-infiltrating cells. Closed bars, tumors from vector-transfected 76-9 cells; open bars, tumors derived from 76-9-P3F-C23 cells. For DC activation analysis, CD11c cells were gated, and respective activation markers were enumerated. Error bars = SEM of four tumors per group.

domain mutant, which has no transcriptional activity on PAX3 targets, had a wild-type effect on DC maturation inhibition (Fig. 4 D). The homeodomain mutant, however, had only ∼40% of the effect on inhibition of DC maturation (Fig. 4 D), which was consistent with a reported role of the homeodomain of PAX3–FKHR in mediating functionally important protein–protein interactions (6, 30). Finally, we confirmed that ARMS cell lines endogenously expressing PAX3–FKHR (RH30 and SCMC) also produce an immunoinhibitory microenvironment that inhibits DC activation in a STAT3-dependent manner, whereas RH18 conditioned media (PAX3–FKHR negative) does not substantially affect DC maturation (Fig. 4 E and not depicted for SCMC). Therefore, PAX3–FKHR interacts with STAT3 to induce secretion of factors that can directly alter local DC activation.

We next analyzed IL-10 secretion from PAX3–FKHR–expressing cells as a candidate cytokine for the PAX3–FKHR–mediated effects on DC maturation. RD cells stably transfected with estrogen-tagged PAX3–FKHR produce increased amounts of IL-10 in a STAT3-dependent manner only in the presence of 4HT, whereas 4HT has no effect on IL-10 production by vector-transfected RD cells (Fig. 4 F). RH30 cells endogenously expressing PAX3–FKHR also produce IL-10 in a STAT3-dependent manner (Fig. 4 F).

PAX3–FKHR suppresses local inflammatory and immunological responses and causes more rapid in vivo growth in immunodeficient mice

To determine if the PAX3–FKHR–induced local cytokine alterations observed in vitro are sufficient to alter host responses to tumors, we analyzed the inflammatory cell infiltrates of subcutaneous tumor xenografts. We have observed in experiments in immunocompetent C57BL/6 mice that growth of PAX3–FKHR–expressing tumors is associated with a specific anti-PAX3 cellular immune response (unpublished data). We therefore performed the initial experiments using $RAG^{-/-}$/common γ chain$^{-/-}$/complement $C5^{-/-}$ mice that have deficiency of functional T cells, B cells, and NK cells (unpublished data). We analyzed intratumoral inflammatory cells by flow cytometry after disaggregating tumors with collagenase. Importantly, the percentage of viable cells was identical between PAX3–FKHR–expressing and –nonexpressing cells so that the percentages of stained cells could be extrapolated to total numbers of infiltrating cells (Fig. 5, middle). We found considerable inhibition of intratumoral DC maturation by PAX3–FKHR and a decrease in infiltration of neutrophils and macrophages (Fig. 5 A). The tumor growth rate of PAX3–FKHR–expressing cells was substantially increased compared with vector-only transfected cells (Fig. 5 A) even though the growth characteristics of the paired cell lines in vitro were identical (not depicted), which was consistent with increased in vivo growth being secondary to decreased tumor inflammatory response.

With engraftment in syngeneic C57BL/6 mice (in which interpretation of tumor growth rate is complicated by the

anti-PAX3 immune response) the presence of PAX3–FKHR was associated with a considerable decrease in the numbers of CD8- and CD4-positive infiltrating T cells and NK cells but no difference in the number of infiltrating total NK1.1-positive cells (NK cells plus NKT cells). These changes were associated with a decrease in the numbers of infiltrating macrophages and neutrophils and a large reduction in the maturation of tumor-infiltrating DCs (Fig. 5 B). The tumor growth rate was identical among PAX3–FKHR–expressing and –nonexpressing tumors.

PAX3–FKHR–expressing ARMS tumors have an immunoinhibitory phenotype

We hypothesized that the rapid growth and local tissue destruction of ARMS should result in marked local inflammation. We analyzed eight PAX3–FKHR–expressing (unpublished data) ARMS primary tumor biopsies and looked for the presence of neutrophils as a marker of inflammation or immune response. We found a mean of only 0.5 neutrophils per 10 high power fields (range 0–2) compared with a mean of 1.5 per 10 ERMS tumors (range 0–4; Fig. 6 A). We next looked at the subcellular location of STAT3 in these same PAX3–FKHR–expressing and –nonexpressing tumor samples by immunohistochemistry using a STAT3-specific antibody. In control tonsil ($n = 1$) and breast carcinoma ($n = 2$) sections, STAT3 was largely cytoplasmic. In three ERMS samples lacking PAX3–FKHR, STAT3 had weak staining
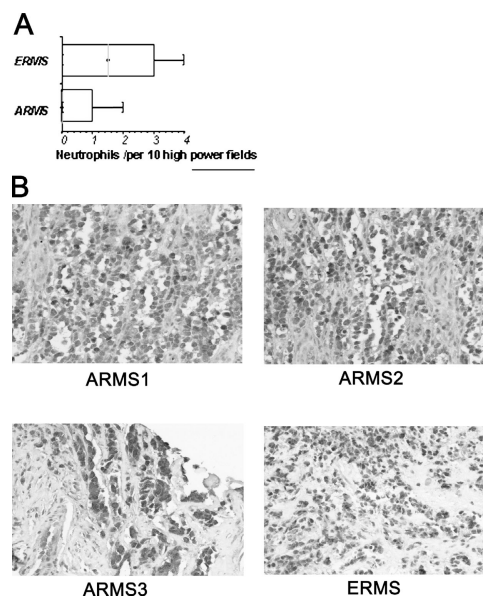

Figure 6.   PAX3–FKHR–expressing ARMS cells have an immunoinhibitory phenotype. (A) Numbers of neutrophils infiltrating PAX3–FKHR–expressing human ARMS versus ERMS tumors. The box whisker plot shows the first and third quartiles, median, and range. (B) Representative image of STAT3 immunohistochemistry of prechemotherapy tumor biopsies or surgical specimens. Three representative ARMS tumors are shown with one ERMS case for comparison.

and was localized in both the cytoplasm and nucleus. (Fig. 6 B). In the ARMS cases, all of which were PAX3-FKHR fusion–positive, there was strong nuclear staining in five out of five cases (Fig. 6 B), indicating high-level expression or stabilization of STAT3 protein and localization in the nucleus.

DISCUSSION

It is well attested in the literature that tumors are capable of inhibiting immunological and inflammatory responses through mechanisms such as the production of the immunoinhibitory cytokine IL-10. Recently, STAT3 has been identified as an immunoinhibitory and oncogenic transcription factor, the activity of which is up-regulated in tumors. Moreover, tumor cells are dependent on STAT3 for growth (29, 31). In this paper, we identify a novel mechanism whereby a chimeric fusion oncoprotein transcription factor (PAX3-FKHR) that is capable of binding target DNA sequences through its DNA binding domain to promote malignant transformation also interacts with STAT3 transcription factor through its FKHR–derived sequences to modify inflammatory response to the developing tumor. The immunomodulatory effect is independent of the ability of the fusion protein to bind PAX3 target promoters, suggesting that PAX3-FKHR might not bind DNA directly when in a transcriptional complex with STAT3. As STAT3 is known to activate genes as both homo- and heterodimers with other STATs, it is likely that there are several different STAT3 target promoter recognition sequences, the binding to which by STAT3 could be differentially regulated by PAX3-FKHR. Further work is needed to identify the pathways by which STAT3 regulates its target promoters and PAX3-FKHR modifies this regulation. The possible physiological significance of the apparent weak interaction between PAX3-FKHR and STAT5 also needs to be tested.

Previous researchers have not identified IFN-γ/IL-6 targets as PAX3-FKHR–negative targets. There are two possible explanations for this. First, in a study by Khan et al. (22), PAX3-FKHR was introduced into NIH3T3 cells that are not myogenic, and the predominant transcriptional pattern identified was up-regulation of a myogenic program. In our study, the recipients are RMS cells already expressing myogenic genes, thereby allowing other transcriptional effects of PAX3-FKHR to be disclosed by microarray analysis. Second, it is possible that JAK/STAT signaling is less active in the cell system used in the study by Khan et al., so the role of PAX3-FKHR interacting with this signaling would be less apparent. We have shown that PAX3-FKHR interacts with STAT3 to alter immunological response to tumors when ectopically expressed in two separate myogenic tumor cell lines. We have also shown that PAX3-FKHR interacts with STAT3 in the physiological setting of RH30 ARMS cells and that blocking STAT3 reverses RH30 cells' inhibition of DCs. Further work is needed to define the mechanism and extent of transcriptional activation and repression by the PAX3-FKHR–STAT3 complex in ARMS cells and tumors

and to define the extent of the contribution, if any, of STAT3 activation to transcription of PAX3-FKHR targets from PAX3 target promoters. However, experimental down-regulation of PAX3-FKHR in ARMS cells to demonstrate reversal of changes in STAT3 targets will be challenging because of the additional survival properties of PAX3-FKHR, which means that its down-regulation results in apoptosis (32, 33).

Previous researchers have demonstrated that unphosphorylated FKHR binds STAT3 and is a cofactor for transcriptional activation of the STAT3 target promoter α2-macroglobulin (26). FKHR activation of STAT3 is negatively regulated by its phosphorylation after AKT activation. It is not known how FKHR differentially interacts with STAT3 and STAT1 homo- and heterodimers. It is interesting to speculate that the normal negative regulation on FKHR by AKT, in terms of its STAT3 coactivation, is missing from the PAX3-FKHR–STAT3 complex because of loss of a critical tyrosine residue in the NH_2 terminus of FKHR. Detailed experimental approaches will be required to determine the target promoters for the PAX3-FKHR–STAT3 complex, whether STAT1 transcription is affected directly or indirectly, and the mechanism of regulation of the complex by upstream signaling. Similarly, the requirement of STAT3 to be phosphorylated in order to be activated when bound by PAX3-FKHR needs to be determined. Two aspects of our data provide some preliminary clues regarding mechanism. First, the presence of PAX3-FKHR seems to be associated with a largely nuclear localization of PAX3-FKHR. Second, PAX3-FKHR lacking PAX3 transcription function has identical effects on DC maturation. These data are consistent with a model in which PAX3-FKHR stabilizes STAT3 in the nucleus and acts (like FKHR) as a transcription activator.

In the in vivo setting we have shown that the PAX3-FKHR–STAT3 interaction causes, in common with STAT3, a marked inhibition of activation of DCs. This inhibition is mediated by secreted factors and is dependent on STAT3 (Fig. 4). The specific STAT3-blocking phosphopeptide used in these experiments functions by binding the SH2 domain and preventing dimerization with other STATs (29), suggesting that PAX3-FKHR, like FKHR (27), may form a complex with STAT dimers to alter STAT transcription. Further work is needed to determine if and how PAX3-FKHR specifically alters transcription of different STAT dimers on different target promoters.

In immunodeficient mice lacking functional B cells, T cells, or NK cells, there is a reduction of macrophage and neutrophil numbers, suggesting inhibition of innate immune responses and inflammation. In this context it is of interest that the presence of PAX3-FKHR is only associated with enhanced tumor growth rates, although growth in vitro is unaffected. A possible explanation for the lack of enhanced growth rate in syngeneic mice is that the presence of PAX3-FKHR itself may paradoxically render the tumors more sensitive to immune detection by cellular anti–PAX3 responses

or NK killing secondary to reduction in MHC expression (unpublished data). Other progrowth factors, such as the STAT3 target VEGF, may also contribute to enhanced growth in the in vivo setting. In future studies, it will be important to show which other oncogenic functions of STAT3 (inhibition of apoptosis, proliferation, inhibition of differentiation, and angiogenesis) are also stimulated by PAX3-FKHR in a STAT3-dependent function. If some or all of these components of the transformed phenotype are active in RMS, then development of agents that specifically block the PAX3-FKHR–STAT3 interaction could be of therapeutic potential with minimal expected toxicity.

We have shown for the first time that an oncogenic fusion protein transcription factor can have a dual function in malignant progression through binding its own target promoters and immune evasion through interaction with JAK-STAT signaling. Down-regulation of MHC and production of immunoinhibitory cytokines such as IL-10 are well known characteristics of tumor cells that are thought to be essential for prevention of inflammation at sites of tissue injury. This in turn might inhibit the detection of tumor-specific antigens, such as fusion oncoproteins themselves. PAX3-FKHR has been recently shown to be an initiating event in ARMS development (9), which suggests that the tumor has, from the time of its initial development, developed sophisticated mechanisms to prevent its own immune detection. If similar mechanisms can be shown to exist in other tumor types, the implication will be that targeting of the critical oncogene could reverse its immune evasion mechanism.

MATERIALS AND METHODS

Plasmids and cloning. The PAX3-FKHR cDNA cloned into pBK-CMV vector has been described previously (8) and is here called pBK-CMV-P3F. PRS9-CAT was a gift from J. Bennicelli (University of Pennsylvania, Philadelphia, PA). The control vectors for transient transfections were pGL3 luciferase, pRL-TK, and pSV-β-galactosidase. P3F-ER was made by cloning the modified estrogen receptor ER (34) to the COOH terminus of PAX3-FKHR in pBK-CMV. For transient transfections of PAX3-FKHR or a truncated PAX3 in 293T cells, the full-length PAX3-FKHR cDNA or PAX3 up to the breakpoint with FKHR had an myc epitope tag added to the COOH terminus and were ligated into a lentivirus vector LNT/SffvMCS/ccdB under the regulation of the WPRE to give high level expression. The PAX3-FKHR mutants G48S and N269 (30) were gifts from F. Barr and J. Xia (University of Pennsylvania, Philadelphia, PA). The Stat3-β construct was a gift from T. Wang (Johns Hopkins University, Baltimore, MD). siRNA targeting STAT3 and corresponding negative control siRNA comprising a mixture of nonspecific target sequences were purchased from Upstate Biotechnology.

Microarray, Northern blotting, and RT-PCR. Total RNA was isolated from triplicate independent cultures of 76-9–CMV, C23, and C24 cells. Preparation of labeled cRNA, hybridization to MG-U74 chips, and scanning were performed according to Affymetrix guidelines (Affymetrix, Inc.). Using Genespring 4.2.1 software, data for each target gene was normalized relative to the gene's mean intensity in 76-9–CMV cells. A filter identified genes that showed greater than a twofold difference in intensity in C23 and C24 relative to the mean intensity of CMV. For Northern blots, total RNA was electrophoresed on 1% formaldehyde agarose gels and transferred to Hybond-N membranes (GE Healthcare) and hybridized in Ultrahyb solution (Ambion) with the relevant radioactively labeled DNA

probe according to the manufacturer's instructions. PAI-1 mRNA expression was determined by quantitative real-time RT-PCR using a genetic analyzer (ABI7000; Applied Biosystems) and an assay (Hs00167155_m1; Applied Biosystems) with relative expression being determined by the comparative method (User Bulletin 2; Applied Biosystems).

Cell culture, stable and transient transfections, and invasion assays. 76-9 cells were maintained in RPMI 1640 media. The human RMS cell lines RH30, RH18, RMS, RD, and SCMC-RM2, as well as 293T, were grown in DMEM supplemented with 10% FCS. To generate stable lines, cells were transfected with Fugene 6 reagent (Roche) and selected in G418 following the manufacturer's protocol. In normalized reporter assays, 1.75 μg of reporter and 0.25 μg of control plasmids were combined. Cells were assayed for reporter activity after 48 h using a CAT ELISA kit (Roche) and β-galactosidase activity (Galacto-Light; Tropix). In some experiments, cells were cultured for 48 h in 20 ng/ml recombinant human IFN-γ (Pepro-Tech). Invasion assays were performed using BioCoat matrigel invasion chambers (Becton Dickinson) according to the manufacturer's instructions.

Western blots and immunoprecipitation. 10^6 cells were lysed in 50 μl of RIPA buffer containing 1 mM sodium orthovanadate and protease inhibitors. Denatured whole cell lysates were electrophoresed and transferred to Hybond-C extra membranes (GE Healthcare) in accordance with the manufacturer's instructions. Membranes were probed with the following primary antibodies: PAI-1 (C-9) mAb (Santa Cruz Biotechnology, Inc.) and α-tubulin mAb (Serotec). All HRP-labeled secondary antibodies were from Santa Cruz Biotechnology, Inc. For immunoprecipitation, 200 μl of lysate from 5 × 10^6 cells was precipitated with 2 μl of anti-STAT3 (rabbit polyclonal antibody; Upstate Biotechnology), anti STATs 2, 4, 5, and 6 (Santa Cruz Biotechnology, Inc.), anti-PAX3 (N19; Santa Cruz Biotechnology, Inc.), or antiestrogen receptor rabbit polyclonal (MC-20; Santa Cruz Biotechnology, Inc.) antibodies using protein A sepharose (GE Healthcare) in accordance with the manufacturer's instructions.

Immunohistochemistry and tissue arrays. Paraffin sections of RMS primary tumors of known PAX3-FKHR status were dewaxed and rehydrated. Endogenous peroxidase was blocked by immersing the sections in 10% hydrogen peroxidase for 20 min at room temperature. Pressure cooking with 10 mM citrate buffer for 4 min was used for the antigen retrieval followed by cooling of the slides for 30 min. The primary polyclonal antibody is prediluted ready to use (Lab Vision). Sections were incubated at room temperature for 60 min. The Envision HRP system for rabbit primary antibodies (DakoCytomation) was used for the detection level. The sections were incubated for 30 min at room temperature. Staining was with diaminobenzidine for 10 min to allow visualization of the antibody.

IL-10 and DC maturation assays. 5 × 10^5 RD P3F-ER cells were plated in a volume of 2 ml, and 1 μM 4HT was added for 48 h to induce PAX3-FKHR function. For DC maturation inhibition experiments, PBMCs were cultured in RPMI 1640 supplemented with 2% human AB serum in the presence of 100 ng/ml GM-CSF and 10 ng/ml IL-4 (both were obtained from PeproTech). 50% of supernatant from tumor cells was added to DC media at day 0. Fresh medium supplemented with supernatants was added to the culture every 2 d until day 4, at which time point 20 ng/ml of KLH was added. DC activation was determined on day 5. For IL-10 assays, cells were induced for 48 h by 1 μM 4HT in the presence or absence of 400 μM of phosphopeptide PY*LKTK (28). IL-10 was detected in supernatants by ELISA (BD Biosciences).

FACS staining and analysis. The following antibodies were used for cell line staining: anti–mouse H-2K^b–PE and anti–mouse H-2D^b–PE (Caltag); anti–human MHC class I (Abcam); and anti–human CXCR-4–PE (clone 12G5; R&D Systems). The following antibodies were used for DC staining: anti-CD86–PE (clone 2331) and anti-HLA–DR–FITC (clone G46-6; BD Biosciences). The following antibodies were used for tumor-

infiltrating cell staining: anti-NK1.1[+] (clone PK136), anti-CD3 (Clone CI-CD3), anti-CD8 (clone RH10), anti-CD4 (clone CI-CD4), anti-F4/80 (clone CI-A3-1), anti-CD11b, (clone M1/70.15), and anti-Ly6G (Gr-1; clone RB6-8C5). For DC staining, the following murine antibodies were used: anti-CD40 (clone 3/23), anti-CD80 (B7-1; clone RMMP-1), and anti-CD86 (B7-2; clone RMMP-3; BD Biosciences). For DC staining, viable and CD11c-positive cells were gated. Stained and fixed (1% paraformaldehyde) cells were analyzed using a FACS machine (Epics; Beckman Coulter) and software (Expo32; Beckman Coulter).

In vivo growth assays. Studies were conducted in 8-wk-old C57BL/6 mice or RAG$^{-/-}$/common γ chain$^{-/-}$/complement C5$^{-/-}$ (RAG$^{-/-}$/CGC$^{-/-}$/C5$^{-/-}$) mice. RAG$^{-/-}$/CGC$^{-/-}$ mice have been described previously (35), and RAG$^{-/-}$/CGC$^{-/-}$/C5$^{-/-}$ mice were generated by backcrossing onto the A/J strain, which is naturally deficient in complement C5. 5×10^6 cells were resuspended in 150 μl sterile PBS and injected subcutaneously with a 26-gauge needle into the flanks of groups of five mice. Tumor size was monitored every 2 d using calipers, and the length (l) and width (w) of the developing tumor were converted to volume using the following equation: vol = (w^2 × l) / 2. Mice were killed when tumors reached a maximum size of 1.5 cm in the largest diameter. Tumors were mechanically disaggregated before staining for flow cytometric analysis.

Online supplemental material. Table I shows the complete list of 35 sequences (derived from 31 different genes) significantly up-regulated by more than twofold in C23 and C24 cells relative to CMV. The asterisks in the left column identify the genes that were also found to be significantly up-regulated by more than 1.5-fold in C23 and C24 cells relative to CMV cells in a higher stringency analysis. Table II shows the complete list of 69 sequences significantly down-regulated by more than twofold in C23 and C24 cells relative to CMV. The asterisks in the left column identify the genes that were also found to be significantly down-regulated by more than 1.5-fold in C23 and C24 cells relative to CMV cells in a higher stringency analysis. Online supplemental material is available at http://www.jem.org/cgi/content/full/jem.20050730/DC1.

REFERENCES

1. McDowell, H.P. 2003. Update on childhood rhabdomyosarcoma. *Arch. Dis. Child.* 88:354–357.
2. Sorensen, P.H., J.C. Lynch, S.J. Qualman, R. Tirabosco, J.F. Lim, H.M. Maurer, J.A. Bridge, W.M. Crist, T.J. Triche, and F.G. Barr. 2002. PAX3-FKHR and PAX7-FKHR gene fusions are prognostic indicators in alveolar rhabdomyosarcoma: a report from the children's oncology group. *J. Clin. Oncol.* 20:2672–2679.
3. Barr, F.G. 2001. Gene fusions involving PAX and FOX family members in alveolar rhabdomyosarcoma. *Oncogene.* 20:5736–5746.
4. Anderson, J., A. Gordon, K. Pritchard-Jones, and J. Shipley. 1999. Genes, chromosomes, and rhabdomyosarcoma. *Genes Chromosomes Cancer.* 26:275–285.
5. Merlino, G., and L.J. Helman. 1999. Rhabdomyosarcoma–working out the pathways. *Oncogene.* 18:5340–5348.
6. Lam, P.Y., J.E. Sublett, A.D. Hollenbach, and M.F. Roussel. 1999. The oncogenic potential of the Pax3-FKHR fusion protein requires the Pax3 homeodomain recognition helix but not the Pax3 paired-box DNA binding domain. *Mol. Cell. Biol.* 19:594–601.
7. Scheidler, S., W.J. Fredericks, F.J. Rauscher III, F.G. Barr, and P.K. Vogt. 1996. The hybrid PAX3-FKHR fusion protein of alveolar rhabdomyosarcoma transforms fibroblasts in culture. *Proc. Natl. Acad. Sci. USA.* 93:9805–9809.
8. Anderson, J., A. Ramsay, S. Gould, and K. Pritchard-Jones. 2001. PAX3-FKHR induces morphological change and enhances cellular proliferation and invasion in rhabdomyosarcoma. *Am. J. Pathol.* 159:1089–1096.
9. Keller, C., B.R. Arenkiel, C.M. Coffin, N. El-Bardeesy, R.A. DePinho, and M.R. Capecchi. 2004. Alveolar rhabdomyosarcomas in conditional Pax3:Fkhr mice: cooperativity of Ink4a/ARF and Trp53 loss of function. *Genes Dev.* 18:2614–2626.
10. Bennicelli, J.L., W.J. Fredericks, R.B. Wilson, F.J. Rauscher III, and F.G. Barr. 1995. Wild type PAX3 protein and the PAX3-FKHR fusion protein of alveolar rhabdomyosarcoma contain potent, structurally distinct transcriptional activation domains. *Oncogene.* 11:119–130.
11. Ginsberg, J.P., R.J. Davis, J.L. Bennicelli, L.E. Nauta, and F.G. Barr. 1998. Up-regulation of MET but not neural cell adhesion molecule expression by the PAX3-FKHR fusion protein in alveolar rhabdomyosarcoma. *Cancer Res.* 58:3542–3546.
12. Fredericks, W.J., N. Galili, S. Mukhopadhyay, G. Rovera, J. Bennicelli, F.G. Barr, and F.J. Rauscher III. 1995. The PAX3-FKHR fusion protein created by the t(2;13) translocation in alveolar rhabdomyosarcomas is a more potent transcriptional activator than PAX3. *Mol. Cell. Biol.* 15:1522–1535.
13. Kerr, I.M., A.P. Costa-Pereira, B.F. Lillemeier, and B. Strobl. 2003. Of JAKs, STATs, blind watchmakers, jeeps and trains. *FEBS Lett.* 546:1–5.
14. Qing, Y., and G.R. Stark. 2004. Alternative activation of STAT1 and STAT3 in response to interferon-gamma. *J. Biol. Chem.* 279:41679–41685.
15. Costa-Pereira, A.P., S. Tininini, B. Strobl, T. Alonzi, J.F. Schlaak, H. Is'harc, I. Gesualdo, S.J. Newman, I.M. Kerr, and V. Poli. 2002. Mutational switch of an IL-6 response to an interferon-gamma-like response. *Proc. Natl. Acad. Sci. USA.* 99:8043–8047.
16. Calo, V., M. Migliavacca, V. Bazan, M. Macaluso, M. Buscemi, N. Gebbia, and A. Russo. 2003. STAT proteins: from normal control of cellular events to tumorigenesis. *J. Cell. Physiol.* 197:157–168.
17. Wang, T., G. Niu, M. Kortylewski, L. Burdelya, K. Shain, S. Zhang, R. Bhattacharya, D. Gabrilovich, R. Heller, D. Coppola, et al. 2004. Regulation of the innate and adaptive immune responses by Stat-3 signaling in tumor cells. *Nat. Med.* 10:48–54.
18. Niu, G., R. Heller, R. Catlett-Falcone, D. Coppola, M. Jaroszeski, W. Dalton, R. Jove, and H. Yu. 1999. Gene therapy with dominant-negative Stat3 suppresses growth of the murine melanoma B16 tumor in vivo. *Cancer Res.* 59:5059–5063.
19. Evans, R., S.J. Kamdar, T. Duffy, and L. Edison. 1993. Intratumor gene expression after adoptive immunotherapy in a murine tumor model. Regulation of messenger RNA levels associated with the differential expansion of tumor-infiltrating lymphocytes. *J. Immunol.* 150:177–184.
20. Shapiro, D.N., B.G. Jones, L.H. Shapiro, P. Dias, and P.J. Houghton. 1994. Antisense-mediated reduction in insulin-like growth factor-I receptor expression suppresses the malignant phenotype of a human alveolar rhabdomyosarcoma. *J. Clin. Invest.* 94:1235–1242.
21. Kalebic, T., M. Tsokos, and L.J. Helman. 1994. In vivo treatment with antibody against IGF-1 receptor suppresses growth of human rhabdomyosarcoma and down-regulates p34cdc2. *Cancer Res.* 54:5531–5534.
22. Khan, J., M.L. Bittner, L.H. Saal, U. Teichmann, D.O. Azorsa, G.C. Gooden, W.J. Pavan, J.M. Trent, and P.S. Meltzer. 1999. cDNA microarrays detect activation of a myogenic transcription program by the PAX3-FKHR fusion oncogene. *Proc. Natl. Acad. Sci. USA.* 96:13264–13269.
23. Gallicchio, M.A., C. Kaun, J. Wojta, B. Binder, and L.A. Bach. 2003. Urokinase type plasminogen activator receptor is involved in insulin-like growth factor-induced migration of rhabdomyosarcoma cells in vitro. *J. Cell. Physiol.* 197:131–138.
24. Pardoll, D. 2003. Does the immune system see tumors as foreign or self? *Annu. Rev. Immunol.* 21:807–839.

JEM

25. Libura, J., J. Drukala, M. Majka, O. Tomescu, J.M. Navenot, M. Kucia, L. Marquez, S.C. Peiper, F.G. Barr, A. Janowska-Wieczorek, and M.Z. Ratajczak. 2002. CXCR4-SDF-1 signaling is active in rhabdomyosarcoma cells and regulates locomotion, chemotaxis, and adhesion. *Blood*. 100:2597–2606.

26. Kortylewski, M., F. Feld, K.D. Kruger, G. Bahrenberg, R.A. Roth, H.G. Joost, P.C. Heinrich, I. Behrmann, and A. Barthel. 2003. Akt modulates STAT3-mediated gene expression through a FKHR (FOXO1a)-dependent mechanism. *J. Biol. Chem*. 278:5242–5249.

27. Barr, F.G., S.J. Qualman, M.H. Macris, N. Melnyk, E.R. Lawlor, D.M. Strzelecki, T.J. Triche, J.A. Bridge, and P.H. Sorensen. 2002. Genetic heterogeneity in the alveolar rhabdomyosarcoma subset without typical gene fusions. *Cancer Res*. 62:4704–4710.

28. Turkson, J., D. Ryan, J.S. Kim, Y. Zhang, Z. Chen, E. Haura, A. Laudano, S. Sebti, A.D. Hamilton, and R. Jove. 2001. Phosphotyrosyl peptides block Stat3-mediated DNA binding activity, gene regulation, and cell transformation. *J. Biol. Chem*. 276:45443–45455.

29. Catlett-Falcone, R., T.H. Landowski, M.M. Oshiro, J. Turkson, A. Levitzki, R. Savino, G. Ciliberto, L. Moscinski, J.L. Fernandez-Luna, G. Nunez, et al. 1999. Constitutive activation of Stat3 signaling confers resistance to apoptosis in human U266 myeloma cells. *Immunity*. 10:105–115.

30. Xia, S.J., and F.G. Barr. 2004. Analysis of the transforming and growth suppressive activities of the PAX3-FKHR oncoprotein. *Oncogene*. 23:6864–6871.

31. Bromberg, J.F., M.H. Wrzeszczynska, G. Devgan, Y. Zhao, R.G. Pestell, C. Albanese, and J.E. Darnell Jr. 1999. Stat3 as an oncogene. *Cell*. 98:295–303.

32. Bernasconi, M., A. Remppis, W.J. Fredericks, F.J. Rauscher III, and B.W. Schafer. 1996. Induction of apoptosis in rhabdomyosarcoma cells through down-regulation of PAX proteins. *Proc. Natl. Acad. Sci. USA*. 93:13164–13169.

33. Ayyanathan, K., W.J. Fredericks, C. Berking, M. Herlyn, C. Balakrishnan, E. Gunther, and F.J. Rauscher III. 2000. Hormone-dependent tumor regression in vivo by an inducible transcriptional repressor directed at the PAX3-FKHR oncogene. *Cancer Res*. 60:5803–5814.

34. Littlewood, T.D., D.C. Hancock, P.S. Danielian, M.G. Parker, and G.I. Evan. 1995. A modified oestrogen receptor ligand-binding domain as an improved switch for the regulation of heterologous proteins. *Nucleic Acids Res*. 23:1686–1690.

35. Goldman, J.P., M.P. Blundell, L. Lopes, C. Kinnon, J.P. Di Santo, and A.J. Thrasher. 1998. Enhanced human cell engraftment in mice deficient in RAG2 and the common cytokine receptor gamma chain. *Br. J. Haematol*. 103:335–342.